



PCCP

**Double-QM/MM Method for Investigating Donor–Acceptor  
Electron Transfer Reactions in Solution**

Journal:	<i>Physical Chemistry Chemical Physics</i>
Manuscript ID:	CP-ART-05-2014-002307.R2
Article Type:	Paper
Date Submitted by the Author:	24-Jul-2014
Complete List of Authors:	Futera, Zdenek; Charles University, Sodeyama, Keitaro; National Institute for Materials Science, International Center for Materials Nanoarchitectonics Burda, Jaroslav; Charles University, Department of Chemical Physics and Optics Einaga, Yasuaki; Keio University, Chemistry Tateyama, Yoshitaka; National Institute for Materials Science, International Center for Materials Nanoarchitectonics

SCHOLARONE™  
Manuscripts

# Double-QM/MM Method for Investigating Donor–Acceptor Electron Transfer Reactions in Solution<sup>†</sup>

Zdenek Futera,<sup>a,b,c</sup> Keitaro Sodeyama,<sup>b,d</sup> Jaroslav V. Burda<sup>e</sup> Yasuaki Einaga<sup>a,c</sup> and Yoshitaka Tateyama<sup>\*b,c,d,f</sup>

Received Xth XXXXXXXXXXXX 20XX, Accepted Xth XXXXXXXXXXXX 20XX

First published on the web Xth XXXXXXXXXXXX 200X

DOI: 10.1039/b000000x

We developed a double–quantum mechanical/molecular mechanical (*d*-QM/MM) method for investigation of full outer–sphere electron transfer (ET) processes between donor and acceptor (DA) in condensed matter. In the *d*-QM/MM method, which employs the novel concept of multiple QM regions, one can easily specify number of electrons, spin states and appropriate exchange–correlation treatment in each QM region, which is especially important in cases of ET involving transition metal sites. We investigated Fe<sup>2+/3+</sup> self-exchange and Fe<sup>3+</sup> + Ru<sup>2+</sup> → Fe<sup>2+</sup> + Ru<sup>3+</sup> in aqueous solution as model reactions, and demonstrated that the *d*-QM/MM method gives reasonable accuracy for the redox potential, reorganization free energy and electronic coupling. In particular, the DA distance dependencies of those quantities are clearly shown at the density functional theory hybrid functional level. The present *d*-QM/MM method allows us to explore the intermediate DA distance region, important for long–range ET phenomena observed in electrochemistry (on the solid–liquid interfaces) and biochemistry, which cannot be dealt by the half–reaction scheme with the conventional QM/MM.

## 1 Introduction

Redox processes – that is, electron transfer (ET) processes – play crucial roles in diverse topics related to energy, environmental and biological issues; catalysis; development of batteries, fuel cells, and solar cells; corrosion; and respiration and photosynthesis. The ET processes involve donor and acceptor (DA) components in condensed–matter systems such as solutions, solid–liquid interfaces, or a group of biological molecules. Typically, transition metal atoms are present as the DA centers. Although many macroscopic applications employing redox processes have been developed, the understanding of ET processes at the atomic and electronic scales remains an issue of great importance. The microscopic implications enable us to design more efficient systems and thus computational methods that can deal with them quantitatively

are desirable. Here, the DA distance dependencies of the redox free energy and the reorganization free energy are the key issues of interest.

As a theory of ET processes, in particular for the outer–sphere ET, Marcus developed the parabolic free–energy concept under the linear–response approximation with respect to the collective solvent response around the DA sites<sup>1,2</sup>. This allows us to calculate the redox and reorganization free energies, which predict the free energy barrier and thus the reaction rate of the ET process. The theory predicted the presence of an inverted region of ET reactions, which was later observed in experiments<sup>3</sup>. The formulation was extended to more general “energy gap” reaction coordinate<sup>2,4</sup> and a number of pioneering classical molecular dynamics (MD) studies<sup>5–8</sup> on the ET between aqueous metal ions have been carried out based on Marcus’ theoretical concept. However, the accuracy of such calculations largely depends on the quality of the force–field potential and its parameters<sup>9–12</sup>. The empirical potential is always a bottleneck for quantitative calculations, and a quantum mechanical description of at least DA centers is desirable.

To overcome the parametrization problem and increase the accuracy of calculations, density functional theory (DFT) together with MD sampling techniques was used to calculate the redox and reorganization free energies of different ET reactions<sup>13–16</sup>. These works are based on the half–reaction computational scheme, in which the donor and acceptor, in contact with the hypothetical electron reservoir, are treated separately. However, this approach is applicable only to dilute limit stud-

<sup>†</sup> Electronic Supplementary Information (ESI) available. See DOI: 10.1039/b000000x

<sup>a</sup> Keio University, 3-14-1 Hiyoshi, Kohoku-ku, Yokohama 223-8522, Japan

<sup>b</sup> International Center for Materials Nanoarchitectonics (WPI-MANA), National Institute for Materials Science (NIMS), 1-1 Namiki, Tsukuba, Ibaraki 305-0044, Japan. E-mail: TATEYAMA.Yoshitaka@nims.go.jp

<sup>c</sup> CREST, Japan Science and Technology Agency (JST), 4-1-8 Honcho, Kawaguchi, Saitama 333-0012, Japan

<sup>d</sup> Elements Strategy Initiative for Catalysts and Batteries, Kyoto University, Goryo-Ohara, Kyoto 615-8245, Japan

<sup>e</sup> Department of Chemical Physics and Optics, Faculty of Mathematics and Physics, Charles University, Ke Karlovu 3, 121 16 Prague 2, Czech Republic

<sup>f</sup> PRESTO, Japan Science and Technology Agency (JST), 4-1-8 Honcho, Kawaguchi, Saitama 333-0012, Japan

ies, and different charges of calculated systems (D vs.  $D^+$  and A vs.  $A^-$ ) require careful treatment of energy that should be aligned to a common reference.

Recently, several DFT-based approaches dealing with full-ET reaction in one simulation box have been developed<sup>17–20</sup>. In these approaches, a constraint of the electronic Hamiltonian was introduced to deal with charge redistribution in the initial (DA) and final ( $D^+A^-$ ) states of the ET reaction. Yet, these calculations are limited by the high demands of the DFT treatment, and adjustment of the constraint still involves some ambiguities. For the latter issue, methods with intrinsic fragmentation of the system may be an appropriate alternative<sup>21</sup>.

As an alternative to the very demanding DFT treatment of the whole system, a combined quantum mechanical/molecular mechanical (QM/MM) technique keeping an accurate quantum mechanical description of DA sites was proposed<sup>22,23</sup>. Zeng *et al.*<sup>23</sup> developed a QM/MM MD method with a fractional number of electrons and demonstrated its feasibility for the ET process between  $Fe^{2+}$  and  $Ru^{3+}$  cations in aqueous solution. However, this QM/MM approach is basically limited to the half-reaction computational scheme because the QM region is usually defined as donor in one simulation box and acceptor in another. While the reorganization free energy is simply sum of the donor and acceptor contribution in the dilute limit, their mutual interaction becomes important in the intermediate DA distance region. To investigate this important region directly by simulation, the full-reaction scheme is necessary. Although some attempts were made to partition the system into more than one QM region surrounded by a MM environment<sup>24–26</sup>, these methods were never applied to ET processes.

In this article, we present a double-QM/MM (*d*-QM/MM) method with independent QM parts that is designed for investigation of intermediate-distance region of outer-sphere donor-acceptor ET reactions in condensed matter using a full-reaction scheme. Note that there are two regimes on the ET processes; the inner-sphere ET with donor-acceptor binding where wavefunction is delocalized over DA and the outer-sphere ET described by Marcus theory, and we focus on the latter in this work. The *d*-QM/MM method allows us to easily specify the number of electrons in the donor and acceptor regions, clearly define their spin states, and choose the most proper exchange-correlation treatment for their charge densities. The donor-acceptor distance dependencies of all ET quantities such as the redox potential, reorganization free energy, and electronic coupling can be evaluated at the first principles level with *d*-QM/MM. Then, we demonstrate the accuracy and performance of the *d*-QM/MM method on  $Fe^{2+/3+}$  cations self-exchange and ET between  $Fe^{2+}$  and  $Ru^{3+}$  cations in aqueous solution, two well known model reactions<sup>6,17,23,27–29</sup>. On the basis of these results, we suggest that the *d*-QM/MM method can be an efficient and reasonably

accurate approach for investigation of distance-dependent ET processes such as reactions at solid-liquid interfaces, which are important in heterogeneous catalysis.

## 2 Theory

In this section we provide brief description of the QM/MM method and introduce its generalization for system partitioning with more than one separated QM part, which we call multiple-QM/MM (*m*-QM/MM). We briefly review Marcus theory of electron transfer in the linear-response approximation together with the energy gap reaction coordinate approach, which provides useful formulas for calculating the redox free energy and reorganization free energy by MD sampling techniques. Finally, we describe calculation of electronic coupling under the two-state approximation since the coupling value is used here to estimate the ET rate constant.

### 2.1 Hybrid QM/MM Computational Technique

Quantitatively accurate description of ET processes requires treating donor and acceptor at the QM level of theory. However, QM calculations are very demanding, and therefore the combined QM/MM method<sup>30</sup> provides an alternative that can be used to reduce computational cost while keeping reasonable accuracy. This is achieved by spatial partitioning of a computational model into an inner part (also often called the QM region, Fig. 1a) and an outer part parametrized by a MM force field. The total QM/MM energy of such a divided system can be formally written as the sum of contributions from both parts and their mutual interaction:

$$E_{\text{QM/MM}}(S) = E_{\text{MM}}(O) + E_{\text{QM}}(I) + E_{\text{QM-MM}}(S). \quad (1)$$

where we denote the inner part as *I*, the outer part as *O*, and the whole system as  $S = I + O$ . The last term in Eq. 1 represents coupling between the parts of the system, and its correct description is crucial for the QM/MM method. However, the total energy can also be reformulated in the so-called subtractive energy scheme:

$$E_{\text{QM/MM}}(S) = E_{\text{MM}}(S) + E_{\text{QM}}(I) - E_{\text{MM}}(I). \quad (2)$$

where the coupling of the inner and outer parts is implicitly involved in subtraction of the MM energy of the inner part from the total MM energy of the whole system<sup>31</sup>. This definition does not require detailed knowledge about the construction of the MM potential, and so it provides a convenient way for coupling external QM and MM program codes. For this reason, we use the subtractive energy formula in the rest of the paper.

In studying outer-sphere ET processes with well-separated donor and acceptor, it is desirable to partition the system into two inner parts, one for the donor and one for the acceptor,

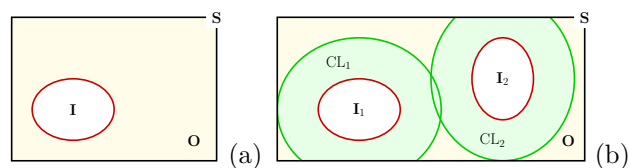


**Fig. 1** Schematic illustration of QM/MM partitioning: (a) conventional QM/MM where the whole system  $S$  is divided into QM inner part ( $I$ ) and MM outer part ( $O$ ), (b) double-QM/MM method with two inner parts surrounded by common outer part. The charge layers (CL) used for electrostatic embedding are shown as green regions.

surrounded by the common outer part. Therefore we generalize Eq. 2 to  $m$ -QM/MM with  $N$  inner parts:

$$E_{\text{QM/MM}}(S) = E_{\text{MM}}(S) + \sum_{i=1}^N [E_{\text{QM}}(I_i) - E_{\text{MM}}(I_i)]. \quad (3)$$

Here we assume that the individual inner parts are not interacting covalently with each other; however, all nonbonding interactions between the inner parts are taken into account. Forces acting on each atom in system  $S$ , which are needed for geometry optimization or MD, can be obtained by differentiation of total energy (3) with respect to the space coordinates:

$$\mathbf{F}_{\text{QM/MM}}(S) = -\nabla E_{\text{MM}}(S) + \sum_{i=1}^N [\nabla E_{\text{MM}}(I_i) - \nabla E_{\text{QM}}(I_i)] \cdot \mathbb{J}_i \quad (4)$$

The Jacobian matrix  $\mathbb{J}_i$  in Eq. 4 transforms the forces from the  $i$ -th inner part into the coordinate system of the whole model  $S$ . This matrix is trivial if there is no chemical bond crossing the boundary between the inner and outer parts.

While the short-range van der Waals interaction is usually described sufficiently well by the MM force field, there are basically two ways to treat the long-range electrostatic interaction. One way, called mechanical embedding, evaluates the Coulombic contribution as a pair interaction between the MM point charges that are assigned to all atoms in the system. This approach requires assigning charges to all atoms in the QM parts. The charge densities of these regions are effectively calculated in a vacuum on geometries extracted from the QM/MM model. To provide a more realistic description, electrostatic embedding can be used where the Coulombic interaction between the inner and outer parts is evaluated at the QM level by inserting MM atomic charges into the QM Hamiltonian,

$$\hat{H}_{\text{QM}}^{\text{e.embd.}} = \hat{H}_{\text{QM}} + \sum_{i=1}^N \int \frac{Z_i \rho(\mathbf{r})}{\mathbf{r}} d\mathbf{r}. \quad (5)$$

The resulting charge densities now reflect their electrostatic environment and are appropriately polarized. The  $m$ -QM/MM method with both mechanical and electrostatic embedding

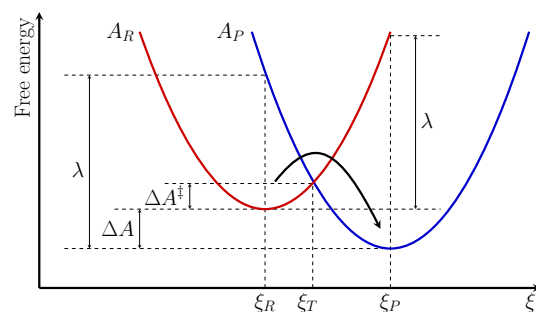


**Fig. 2** Marcus parabolic free energy surfaces of reactant ( $A_R$ ) and product ( $A_P$ ) with indicated redox free energy  $\Delta A$ , reorganization free energy  $\lambda$  and the free energy barrier  $\Delta A^\ddagger$  of outer-sphere ET reaction.

was implemented in our new software, called QMS (see Supporting Information for details).

## 2.2 Electron Transfer Theory

Marcus theory provides the basic theoretical description of electron transfer reactions in the linear-response approximation. The free energy surfaces of the donor and acceptor are assumed to have parabolic shapes with the same curvatures (schematically shown in Fig. 2). The redox free energy, or driving force, of an ET reaction ( $\Delta A$ ) is the free energy difference between the reactants and products of the reaction,

$$\Delta A = A_P(\xi_P) - A_R(\xi_R). \quad (6)$$

The curvature of the parabolas, i.e., the steepness of the free energy surface around minima, is described by the reorganization free energy  $\lambda$ , which is the energy needed for relaxation of the system when nonadiabatic Frank-Condon ET transition between two surfaces occurs:

$$\lambda = A_P(\xi_R) - A_P(\xi_P) = A_R(\xi_P) - A_R(\xi_R). \quad (7)$$

This relatively simple description leads to the well-known Marcus formula for activation free energy

$$\Delta A^\ddagger = \frac{(\Delta A + \lambda)^2}{4\lambda}. \quad (8)$$

From a computational viewpoint, it is convenient to define the reaction coordinate of the system as an energy gap between the initial and final states,  $\xi = \Delta E(\mathbf{R}^N) = E_P(\mathbf{R}^N) - E_R(\mathbf{R}^N)$ , as first introduced by Warshel<sup>4</sup>.  $E_R$  and  $E_P$  might be the reduced state and oxidized state, respectively, of a species in the half-reaction formalism, or  $DA$  and  $D^+A^-$  pairs in the full reaction approach. The gap is evaluated on identical structure coordinates  $\mathbf{R}^N$  and the free energy changes can be obtained by thermodynamic integration.<sup>16</sup> Within linear-response theory this integration can be easily evaluated by trapezoidal rule

that leads to following formulas for the redox and reorganization free energies:<sup>14</sup>

$$\Delta A(\mathbf{R}^N) = \frac{1}{2} (\langle \Delta E(\mathbf{R}^N) \rangle_R + \langle \Delta E(\mathbf{R}^N) \rangle_P), \quad (9)$$

$$\lambda(\mathbf{R}^N) = \frac{1}{2} (\langle \Delta E(\mathbf{R}^N) \rangle_R - \langle \Delta E(\mathbf{R}^N) \rangle_P), \quad (10)$$

where  $\langle X \rangle_s$  notation means statistical average of variable  $X$  on potential surface  $s$ .

The reorganization free energy characterizes the response of the molecular environment of the DA centers to charge changes on these sites. This energy can be separated into two contributions, one from molecules in the inner part and the other from the solvent in the outer part,  $\lambda = \lambda_{in} + \lambda_{out}$ . As derived by Marcus<sup>32,33</sup> from the dielectric continuum model in the linear response approximation,  $\lambda_{out}$  depends on the mutual distance of the electron donor and acceptor,  $R_{DA}$ :

$$\lambda_{out}(R_{DA}) = \left( \frac{1}{\epsilon_o} - \frac{1}{\epsilon_s} \right) \left( \frac{1}{2r_D} + \frac{1}{2r_A} - \frac{1}{R_{DA}} \right) (\Delta q)^2. \quad (11)$$

In this expression,  $r_D$  and  $r_A$  are the effective Born radii of the solutes and  $\Delta q$  represents the transferred charge. Solvent properties are characterized by the Pekar factor  $1/\epsilon_o - 1/\epsilon_s$ , which is difference of its reciprocal high-frequency (optical) dielectric constant and the reciprocal static dielectric constant. The validity of this expression, which is important for quantitative studies of distance-dependent electrode reaction, has been explored by a number of researchers<sup>34–39</sup> and it can be directly verified by our  $d$ -QM/MM method. From the expression (11) it follows that in dilute limit  $\lambda_{out}$  is the sum of the donor and acceptor contributions, which is often exploited in the half-reaction scheme to calculate the total reorganization free energy.

The free energy barrier  $\Delta A^\ddagger$ , which is distant dependent through  $\lambda(R_{DA})$ , is an important quantity for the kinetics of ET reactions. The semi-classical Marcus theory in the linear-response regime gives the following expression for the first-order ET rate:

$$k_{ET} = \frac{2\pi}{\hbar} |V_{DA}|^2 \frac{1}{\sqrt{4\pi\lambda k_B T}} \exp \left[ -\frac{\Delta A^\ddagger}{k_B T} \right]. \quad (12)$$

The strength of the interaction between donor and acceptor in their transition-state configurations, which is responsible for the energy splitting around the intersection region of Marcus parabolas, is measured by electronic coupling element  $V_{DA}$ . In this work, we use a two-state model for approximate evaluation of the coupling<sup>40</sup>

$$V_{DA} = \frac{1}{1 - S_{DA}^2} \left| H_{DA} - \frac{1}{2} S_{DA} (H_{DD} + H_{AA}) \right|, \quad (13)$$

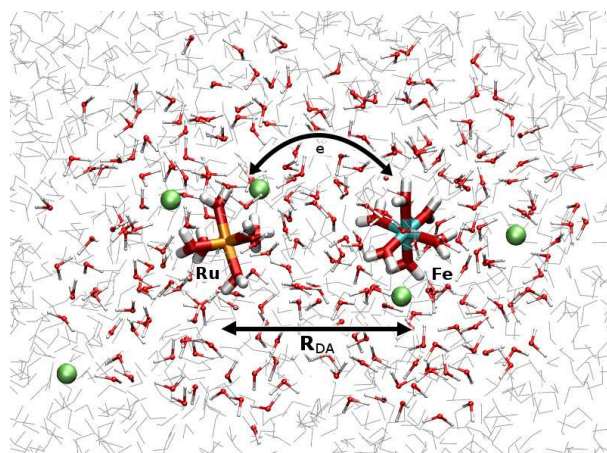


**Fig. 3** A snapshot from the trajectory of the double-component model with a Ru–Fe separation of 10 Å. Metal cations and their first hydration shells (shown in licorice graphical representation) are defined as QM inner parts of the system. These are surrounded by MM water, and 5 chlorine anions (green balls) are used to compensate the positive charge of the complexes. The highlighted water molecules represent the charge layer used for the inner-parts electronic polarization in electrostatic embedding.

where  $S_{DA}$  and  $H_{DA}$  are matrix elements of the overlap and Hamiltonian matrices between the highest occupied molecular orbital (HOMO) of the donor and the lowest unoccupied molecular orbital (LUMO) of the acceptor.

### 2.3 Computational Details

To demonstrate the performance of the  $d$ -QM/MM method, we investigated a model self-exchange ET reaction between the  $\text{Fe}^{2+/3+}$  couple in aqueous solution and also we explored the heterogeneous ET in the  $\text{Fe}^{2+} + \text{Ru}^{3+}$  cation pair in the same medium. These metal ions interact relatively strongly with nearest water molecules. Therefore we define two inner parts of a system as these two cations and their first hydration shells. Surrounding outer part is formed by an explicit TIP3P water box<sup>41</sup> that includes chloride counterions compensating the positive charge of the cations (see Fig. 3). The energies of the inner parts were evaluated by a hybrid B3LYP functional with a localized 6-31G(d) basis set and Stuttgart–Dresden (SDD) pseudopotentials<sup>42–44</sup> on metal centers. Unrestricted DFT calculations were performed for high-spin-state iron and low-spin-state ruthenium electron configurations because these are energetically the most stable. Since we are using the subtractive QM/MM energy scheme, the inner parts were parametrized by GAFF<sup>45</sup> with fitted RESP atomic charges<sup>46,47</sup>. Specific parameters of computational models for standard, single, QM/MM ( $s$ -QM/MM) and  $d$ -QM/MM calculations are described in Supporting Information.

One of the advantages of the present outer-sphere full-reaction approach is the capability to check the dependencies of  $\Delta A$  and  $\lambda$  on the DA separation distance  $R_{DA}$ . Therefore, we ran 30 independent sets of *d*-QM/MM MD calculations to span the distance interval between 6 and 20 Å, representing the touching-part limit and the dilute limit, respectively. These MD runs, each 20 ps long, were calculated for both  $\text{Fe}^{2+} + \text{Ru}^{3+}$  and  $\text{Fe}^{3+} + \text{Ru}^{2+}$  pairs, and the ET energy gap was sampled every 10 fs together with the electronic coupling value. Data from all windows were then collected and used for construction of the  $\Delta A(R_{DA})$ ,  $\lambda(R_{DA})$ , and  $\Delta A^\ddagger(R_{DA})$  curves discussed below. Self-exchange ET on the  $\text{Fe}^{2+/3+}$  pair was checked for the touching-part limit and dilute limit only. All calculations were performed by our own software, called QMS, which couples the program Gaussian 09<sup>48</sup> with the Amber 11 MM package<sup>49</sup> to perform QM/MM MD simulations. More details about the QMS program can be found in the Supporting Information.

In this work, we used standard TIP3P water model without polarization because we would like to compare our results with the published conventional QM/MM data<sup>23</sup> for the same system. It is well known that the lack of polarization leads to overestimation of the reorganization energy<sup>50,51</sup>. Nevertheless, this systematic error in  $\lambda$  can be empirically corrected for comparison with experimental data. The polarizable force field can be straightforwardly applied in *d*-QM/MM and we will demonstrate it in our future work.

### 3 Results and Discussion

Many classical MD studies of ET reactions between metal ions in water<sup>4,6,9,52,53</sup> have been performed; however, accurate quantitative agreement has not been achieved with classical force-fields. The reorganization free energy  $\lambda$  for the aqueous  $\text{Fe}^{2+/3+}$  self-exchange reaction was calculated to be 3.6 eV for ions 5.5 Å apart<sup>6</sup>, whereas experimentally<sup>29</sup> (at the slightly shorter separation of 5.32 Å),  $\lambda$  was found to be 2.1 eV. Several studies of ET reactions including electronic polarization in classical force-field potentials have been done<sup>10,52</sup>. However, at least donor and acceptor description at the QM level of theory is required for realistic and quantitative calculations of ET processes<sup>23</sup>. Recently, accurate results were reached with full first-principle methods<sup>17,20,21,54</sup>. Here, we demonstrate that the *d*-QM/MM method for outer-sphere full-reaction studies of ET processes is a reasonably accurate and efficient alternative to these methods.

Initially we show that our *d*-QM/MM method is consistent with the conventional QM/MM method (*s*-QM/MM) in the dilute limit. For this purpose, we use the model of  $\text{Fe}^{3+} + \text{Ru}^{2+} \rightarrow \text{Fe}^{2+} + \text{Ru}^{3+}$  ET reaction with constrained intermetallic distance at  $R_{DA} = 20$  Å. This system was previously studied by Zeng *et al.*<sup>23</sup> by *s*-QM/MM using the fractional electron

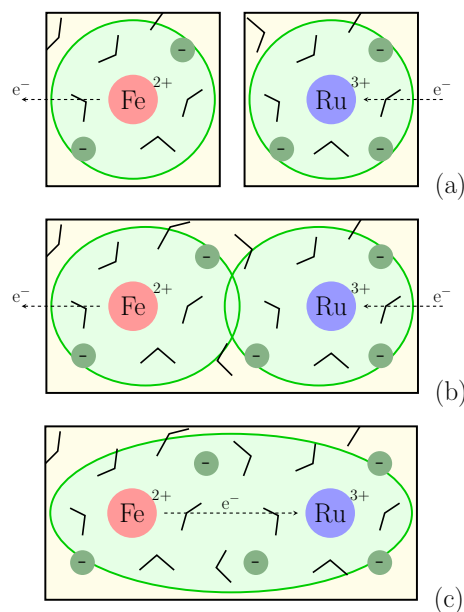


**Fig. 4** Schematic illustration of three different computational schemes applied to the  $\text{Fe}^{3+} + \text{Ru}^{2+} \rightarrow \text{Fe}^{2+} + \text{Ru}^{3+}$  ET process studied in this work. Green regions represent the charge layers used in electrostatic embedding to polarize the inner parts of the system. (a) half-reaction scheme in *s*-QM/MM, (b) half-reaction scheme simulated in *d*-QM/MM by charge layers analogous to those used in *s*-QM/MM, (c) full-reaction scheme in *d*-QM/MM.

approach, and thus we can use it as a reference system. First we use the mechanical embedding approach to calculate the redox free energy and reorganization free energy according to (9) and (10). In this approximation, the obtained values are practically the same in both *s*-QM/MM and *d*-QM/MM (Table 1). The redox free energy calculated at the B3LYP level, -1.0 eV, is considerably overestimated compared to the expected value of -0.68 eV obtained in Ref.<sup>23</sup>, probably because of the chosen calculation conditions of the metal centers and their first hydration shells, as discussed below. Reorganization free energy of 4.0 eV obtained by *d*-QM/MM in dilute limit is consistent with our *s*-QM/MM result. The long-range electrostatic interaction between donor and acceptor is completely screened by bulk water for the dilute limit case  $R_{DA} = 20$  Å, and thus the full-reaction *d*-QM/MM description leads to the values consistent with the half-reaction *s*-QM/MM approach.

Next we apply the electrostatic embedding approach for treatment of the Coulombic interaction. To reach consistency between *s*-QM/MM and *d*-QM/MM, 2 or 3 nearest counterions must be involved in charge layers around the  $\text{M}^{2+/3+}$  ( $\text{M} = \text{Fe}, \text{Ru}$ ) cations. In this way, the half-reaction scheme is simulated in the *d*-QM/MM method; i.e., the electron is exchanged between the cation and the virtual reservoir that is in thermal equilibrium with the system. The half-reaction *s*-QM/MM

computational approach is compared with  $d$ -QM/MM in the half- and full-reaction computational schemes in Fig. 4, where the charge layers are indicated by green boundaries. For the half-reaction scheme is typical that the net charge of each inner part and its charge layer is changed during the energy gap  $\Delta E$  evaluation. This approach improves value of the redox free energy to  $-0.8$  eV and it leads to the reorganization energy  $4.7 - 4.9$  eV, consistent with  $4.9$  eV published in Ref. <sup>23</sup> when we consider the total  $\lambda$  as a sum of inner ( $\lambda_{in}$ ) and outer ( $\lambda_{out}$ ) part contributions of both metals,  $\lambda = \lambda_{in}^{Fe} + \lambda_{out}^{Fe} + \lambda_{in}^{Ru} + \lambda_{out}^{Ru}$ .

However, the  $d$ -QM/MM method is designed for the full-reaction scheme, in which these charge inconsistencies are avoided by including all the counterions together with the donor (acceptor) in the charge layers around the acceptor (donor). The charge density of the second QM inner part is represented simply by point charges involved in the charge layer of the first QM inner part and vice versa. This computational scheme yields  $\lambda = 4.1$  eV, which is consistent with the mechanical embedding result, as one would expect because the reorganization free energy reflects the behavior of the solvent that is modeled by the TIP3P model in both cases. Reorganization free energies of inner parts (first hydration shells of the cations) are  $\lambda_{in}^{Ru} = 0.29$  eV and  $\lambda_{in}^{Fe} = 0.41$  eV, and these values are consistent with  $0.35$  eV and  $0.38$  eV obtained by Zeng *et al.*<sup>23</sup>. The redox free energy  $\Delta A = -0.9$  eV is slightly improved compared to the mechanical embedding result because in electrostatic embedding the electron density of each metal-complex is polarized by charges of the surrounding solvent molecules. The effect is not large since the first hydration shell is described at the QM level together with each cation, and thus the electrostatic interaction between the metal center and more-distant solvent molecules is effectively screened. The consistency between the mechanical and electrostatic embedding approaches as well as their convergence to the  $s$ -QM/MM results for large separation distance  $R_{DA}$  demonstrates the good performance of the  $d$ -QM/MM method. The convergence is also confirmed in the distance dependent profiles of  $\Delta A$  and  $\lambda$ , which is further discussed below.

To gain insight into the energy decomposition of the  $Fe^{3+}$

	Mechanical embedding		Electrostatic embedding		
	$s$	$d$	$s$	$d_{half}$	$d_{full}$
$\Delta A$	-1.08	-1.07	-0.78	-0.87	-0.91
$\lambda$	4.01	4.04	4.89	4.71	4.09
$\Delta A^\ddagger$	0.54	0.55	0.86	0.78	0.62

**Table 1** Comparison of  $s$ -QM/MM with  $d$ -QM/MM in the dilute limit  $R_{DA} = 20$  Å. (a) mechanical embedding, (b) electrostatic embedding where  $d$ -QM/MM was used in half-reaction ( $d_{half}$ ) and full-reaction scheme ( $d_{full}$ ), respectively.

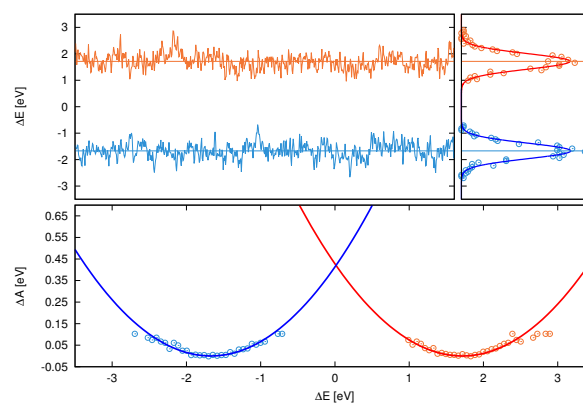


**Fig. 5** Trajectory of energy-gap reaction coordinate [eV] for  $Fe^{2+/3+}$  cations  $6.0$  Å apart (left upper part), corresponding histograms fitted by Gaussian functions (right upper part) and constructed diabatic free energy surfaces (lower part).

+  $Ru^{2+} \rightarrow Fe^{2+} + Ru^{3+}$  ET process, we estimated  $\Delta A$  and  $\lambda$  in the dilute limit from the QM part energies only. In contrast to the results based on the total QM/MM energy differences and MD sampling discussed above, for simplification, the energy decomposition here was done on a representative optimized structure. The calculated ionization energies are listed in Tables S5 and S6 of the Supporting information. In mechanical embedding, there should be no difference between  $s$ -QM/MM and  $d$ -QM/MM at the dilute limit because electrostatic interaction with the solvent is calculated completely at the MM level in these approaches. Indeed, there are only small differences in the calculated values of the redox energy and reorganization energy obtained by the two methods. The discrepancies are attributed to the different geometries of the optimized structures, and these discrepancies would disappear if we applied MD sampling techniques. The QM inner part energies in mechanical embedding directly lead to the inner part reorganization energy mentioned above. In contrast, the electrostatic embedding approach provides information about the total reorganization energy even at the QM level because the interaction with the solvent is involved. The resulting  $\lambda = 4.1$  eV is consistent with the value obtained from the total QM/MM energies. The redox energy is practically the same in both charge embedding approaches. From these results, it is evident that the redox energy is fully controlled by the electronic states of the metal centers and interaction with their first hydration shells, whereas the reorganization free energy is influenced by a larger amount of surrounding solvent.

Before we investigate the distance-dependent behavior of the studied ET between iron and ruthenium, we examined the performance of the  $d$ -QM/MM method close to the touching-part limit. This is the short-distance region where the two QM inner parts become interact directly one to each other

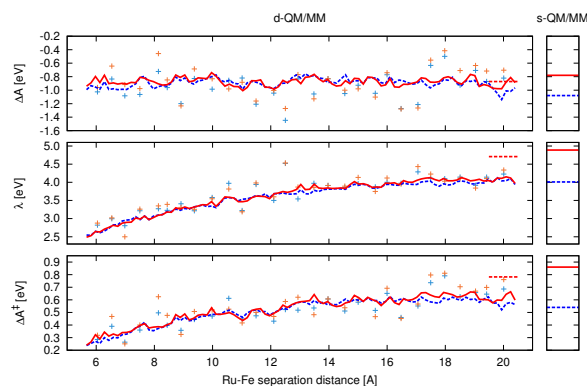


**Fig. 6**  $\Delta A(R_{DA})$ ,  $\lambda(R_{DA})$  and  $\Delta A^\ddagger(R_{DA})$  obtained from  $d$ -QM/MM MD. Mechanical embedding (blue) and electrostatic (red) embedding are compared. Cross marks represent values from energy-minimized structures. Red dashed lines indicate the dilute limit with 2/3 counterions in the charge layer, which is consistent with the  $s$ -QM/MM result shown in the right part of the plot.

and in our case the touching-part limit coincide also with the limit of Marcus outer-sphere regime. We explored the self-exchange ET of the  $\text{Fe}^{2+}$ – $\text{Fe}^{3+}$  pair, a well known model system, to demonstrate reliability of  $d$ -QM/MM. We constructed diabatic free energy surfaces of these two cations 6 Å apart, the distance close to the experimentally suggested limit  $R_{DA} = 5.5$  Å<sup>6,17,29</sup>. The extrapolated parabolic surfaces yielded a reasonable free energy barrier  $\Delta A^\ddagger = 0.42$  eV (Fig. 5), although the cross-section region was not sampled. The obtained barrier corresponds to the reorganization free energy  $\lambda = 1.68$  eV because in the case of self-exchange ET reactions the barrier is simply  $\lambda/4$ . The obtained value of  $\lambda$  is significantly lower than 2.8 eV estimated by Zeng *et al.*<sup>23</sup> from  $s$ -QM/MM data. This demonstrates the full-reaction scheme effect that yields lower value of  $\lambda$  in electrostatic embedding as was discussed above. On the other hand, the obtained value is still rather low compared to 2.1 eV measured experimentally<sup>29,55</sup>. A more accurate description could be obtained by better sampling of the reaction coordinate around  $\Delta E = 0$ . Based on the results discussed so far, we conclude that the  $d$ -QM/MM method can be used as a tool for investigating ET processes in the Marcus regime.

One of the main advantages of the full-reaction computational approach, for which the  $d$ -QM/MM method is designed, is the capability to investigate the  $R_{DA}$  dependence of all ET quantities. We constructed distance-dependent redox free energy  $\Delta A(R_{DA})$  and reorganization free energy  $\lambda(R_{DA})$  curves for the  $\text{Fe}^{3+} + \text{Ru}^{2+} \rightarrow \text{Fe}^{2+} + \text{Ru}^{3+}$  ET reaction over the whole distance range between the touching-part and dilute limits. Both quantities, together with the resulting free energy activation barrier  $\Delta A^\ddagger$  are shown in Fig. 6, where  $s$ -QM/MM values are shown on the right-hand side for comparison. Be-

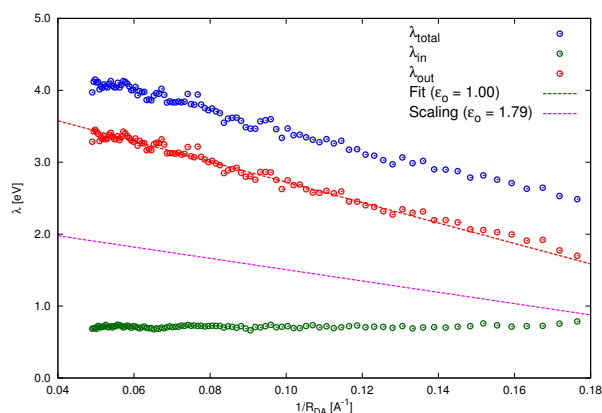


**Fig. 7** Decomposition of the reorganization free energy  $\lambda(R_{DA})$  to its inner part  $\lambda_{in}(R_{DA})$  and outer part  $\lambda_{out}(R_{DA})$  contributions.  $\lambda_{out}$  was fitted by Marcus expression 11 with  $\epsilon_o = 1.0$ . Rescaling of  $\lambda_{out}$  to  $\epsilon_o = 1.79$ , reflecting the solvent polarization, is shown as well.

cause  $\Delta A$  is governed by the electronic states of the metal centers and is affected mainly by their first hydration shells, the redox free energy remains practically constant, fluctuating around the mean value of -0.88 eV. The average configuration of the first hydration shells is kept for  $R_{DA}$  larger than the touching-part limit. Below this limit, deviation from the constant value of  $\Delta A$  can be expected because metallic centers become sufficiently close for direct electronic interaction and the outer-sphere description of ET is there not appropriate. However, such close contact is prevented by electrostatic repulsion of the cations, which is balanced at longer distances by interaction with counterions. In contrast to  $\Delta A$ ,  $\lambda(R_{DA})$  increases from the touching-part limit (2.4 eV) as the number of solvent molecules affected by change of the electrostatic field increases.

In the QM/MM formalism, we can easily decompose the total reorganization energy  $\lambda$  to its inner part  $\lambda_{in}$  and outer part  $\lambda_{out}$  contributions. This decomposition of  $\lambda$  is shown in Fig. 7 where the reorganization energy is plotted on a reciprocal distance scale. As expected,  $\lambda_{in}$  is practically independent of  $R_{DA}$  since its value results from a structural arrangement and vibrations only of the first hydration shell of the cations. In contrast,  $\lambda_{out}$  depends linearly on  $R_{DA}^{-1}$ , which is consistent with formula (11) derived by Marcus for a spherical donor and acceptor in a continuum solvent. By fitting the calculated data to Eq. 11 we obtained a donor (acceptor) radius of 3.83 Å when we used optical dielectric constant  $\epsilon_o = 1.0$ , corresponding to a nonpolarizable solvent. For better model of aqueous solution, we can estimate the effect of the polarization by empirical scaling of the reorganization energy to a Pekar factor for  $\epsilon_o = 1.79$  as was suggested in Ref.<sup>56</sup>. This leads to a dramatic reduction of  $\lambda$ , which is known to be overestimated in calculations without polarization<sup>50</sup>. For instance, the total re-

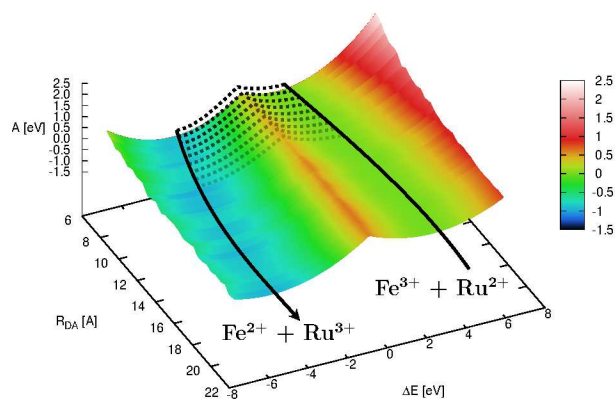


**Fig. 8** Reconstructed free energy surface  $A(R_{DA}, \Delta E)$  for the  $\text{Fe}^{3+} + \text{Ru}^{2+} \rightarrow \text{Fe}^{2+} + \text{Ru}^{3+}$  ET reaction. The minimum free energy path is shown by a thick black arrow. Dotted lines below 10 Å indicate the region where crossing the barrier is probable.

organization free energy is reduced from 4.1 eV to 2.6 eV in the dilute limit. The experimental value, 3.65 eV<sup>55,57</sup>, lies in this calculated range.

Using the calculated profiles of  $\Delta A(R_{DA})$  and  $\lambda(R_{DA})$ , we reconstructed a two-dimensional free energy surface  $A(R_{DA}, \Delta E)$  of the  $\text{Fe}^{3+} + \text{Ru}^{2+} \rightarrow \text{Fe}^{2+} + \text{Ru}^{3+}$  reaction (8). The surface consists of two Marcus parabolas that are vertically shifted by  $\Delta A$  and intersect on the  $\Delta E = 0$ , line where the free energy barrier of the reaction is located. This barrier is gradually lowered as  $R_{DA}$  decreases (see lower part of Fig. 6), and finally the two diabatic surfaces become degenerate below the touching-part limit. Fig. 8 shows the minimum free energy path of the reaction, which corresponds to the most probable pathway of the ET process. In detail, the  $\text{Fe}^{3+}$  and  $\text{Ru}^{2+}$  ions approach each other from the dilute limit, coming into close contact where the barrier is sufficiently low for electron tunneling and ET to occur, and the resulting  $\text{Fe}^{2+}$  and  $\text{Ru}^{3+}$  ions diffuse apart from one another. Although we could not reach the degenerate region below the touching-part limit and did not take into account the electrostatic repulsion of the two cations, the free energy surface is in qualitative agreement with the  $\text{Ru}^{2+/3+}$  self-exchange reaction studied in the full first-principle approach by Oberhofer and Blumberger<sup>58</sup>.

Finally, we evaluated the electronic coupling  $V_{DA}$  in addition to the Franck-Condon parameter to estimate the value of rate constant. The coupling was calculated in the two-state approximation on all MD samples. The  $R_{DA}$  dependence of  $V_{DA}$  over the distance range 6 to 20 Å is shown in logarithmic scale in Fig. 9. Fig. 9b clearly shows that  $V_{DA}(R_{DA})$  exponentially decays and that it is linearly dependent on the overlap between the two frontier molecular orbitals. By fitting the obtained values to  $f(R_{DA}) = \alpha \exp[-\beta R_{DA}]$ , we obtained the decay factor  $\beta = 1.36 \text{ \AA}^{-1}$ , indicating the short-range ET

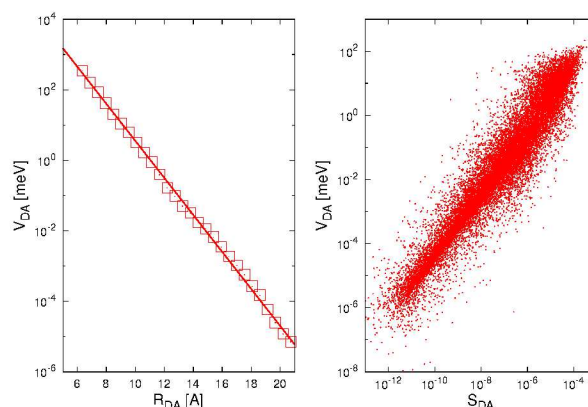


**Fig. 9** Electronic coupling  $V_{DA}$  between the HOMO of the donor and the LUMO of the acceptor. (a) distance dependence of  $V_{DA}$  and (b) dependence of  $V_{DA}$  on overlap  $S_{DA}$ .

character of the reaction. This value is consistent with the value of  $1.23 \text{ \AA}^{-1}$  calculated for  $\text{Ru}^{2+/3+}$  self-exchange<sup>59</sup>, although the MM calculation value for analogous  $\text{Fe}^{2+/3+}$  self-exchange,  $2.31 \text{ \AA}^{-1}$ , is considerably larger<sup>6</sup>. Using the calculated  $\Delta A$  and  $\lambda$ , we estimated a  $k_{DA}$  rate constant of  $2.3 \cdot 10^{-5} \text{ s}^{-1}$  at the touching-part limit 5.5 Å, which rapidly decays to zero with increasing  $R_{DA}$  ( $9.5 \cdot 10^{-15}$  at 10 Å).

Taking into account the polarization effect by empirical scaling of  $\lambda$ , the free energy barrier  $\Delta A^\ddagger$  reduces from 0.24 eV to 0.08 eV at touching-part limit and the estimated  $k_{DA}$  becomes  $5.2 \cdot 10^1 \text{ s}^{-1}$ , close to the experimentally measured  $7.9 \cdot 10^2 \text{ s}^{-1}$ <sup>29</sup>. For exchange-correlation treatment, the global hybrid functionals fail to describe the ET phenomena at one-electron level because of their incorrect asymptotic behavior. Therefore, the long-range-corrected functionals, where the DFT exchange part is continuously substituted by the exact HF exchange at long distances, are expected to yield more accurate results<sup>60–62</sup>. We examined the touching part limit by LC-BLYP and wb97XD functionals with LANL08 metal pseudopotentials (see Supporting Information). These give moderately improved  $\Delta A$  values while the reorganization free energy  $\lambda$  slightly increases in both cases. Nevertheless, the correct asymptotic behavior of the exchange part surely improves the value of  $V_{DA}$  that is increased by one order in case of LC-BLYP whereas it remains practically unchanged for wb97XD. For the rate constant, the increase of the free energy barrier  $\Delta A^\ddagger$  is the dominant effect and thus  $k_{DA}$  is lowered by two orders. We can see that the reaction rate constant is very sensitive quantity and more accurate calculations of  $\Delta A$  and  $\lambda$  are necessary for its determination.

To stress the importance of proper spin state control in transition metal DA centers, we evaluated  $\Delta A$  and  $\lambda$  of the target reaction in the dilute limit also with the low-spin-state Fe complex (Table 2). The value of the redox free energy in

low spin–state case,  $-1.18$  eV differs markedly from that in the high–spin–state case,  $-0.88$  eV, which is more consistent with the experimental value of  $-0.54$  eV. This  $\Delta A$  value reflects the chosen exchange–correlation treatment of the QM inner parts, the B3LYP functional with SDD pseudopotentials in our case. In contrast, the reorganization free energy, which is mainly a property of solvent, remains around  $4.1$  eV. In the  $d$ -QM/MM method, both QM inner part description and solvent parameters can be tuned to the desired level to describe a particular system, and therefore the  $d$ -QM/MM method can be a useful tool for investigating various outer–sphere ET processes.

## 4 Conclusion

We have presented a novel multiple quantum–mechanics/molecular–mechanics method ( $m$ -QM/MM method) as a generalization of the conventional QM/MM method. The  $m$ -QM/MM method enables partitioning of a particular system into separate QM inner parts surrounded by a MM force–field molecular environment. Here, we demonstrated application of  $m$ -QM/MM with two QM inner parts, double–QM/MM ( $d$ -QM/MM), on investigation of an outer–sphere ET process between donor and acceptor. DA spin–charge densities can be easily controlled in this method by appropriate choice of their exchange–correlation treatment. In contrast to the  $s$ -QM/MM approach, which is applicable only in the half–reaction scheme, the  $d$ -QM/MM method enables us to study outer–sphere ET reactions in the full–reaction scheme. Thus not only the dilute limit but also distance dependent phenomena of the ET processes can be explored, in particularly in the intermediate DA distance region.

We have shown the performance of the  $d$ -QM/MM method by studying the well–known  $\text{Fe}^{2/3+}$  cation self–exchange and the  $\text{Fe}^{3+} + \text{Ru}^{2+} \rightarrow \text{Fe}^{2+} + \text{Ru}^{3+}$  ET reaction in explicit aqueous solution. For these we calculated the redox free energy, reorganization free energy and electronic coupling over the whole distance range from the touching–part limit to the

dilute limit. Here, each metal cation surrounded by 6 nearest water molecules was treated at the QM level while the solution environment was simulated by a large amount of MM water. We showed that  $d$ -QM/MM is consistent with  $s$ -QM/MM in the dilute limit and that it provides reasonable accuracy in the touching–part limit as well. The redox free energy as a property of metal center electronic states remains practically unchanged above the touching–part limit, whereas the reorganization free energy follows the Marcus formula and increases monotonically to the dilute limit value. Effect of the solvent electronic polarization on  $\lambda$  was estimated by the empirical scaling approach. The rate constant of the studied ET process was estimated from calculated Frank–Condon factor and exponentially decaying electronic coupling factor. On the basis of our results, we believe that the  $d$ -QM/MM method has the potential to be a powerful tool for investigating a large variety of outer–sphere ET reactions, especially distance–dependent processes at solid–solution interfaces, which are important in electrochemistry, heterogeneous catalysis, and biochemistry.

## Acknowledgements

This work was partly supported by KAKENHI 20540384 and 23340089 as well as by the Strategic Programs for Innovative Research (SPIRE), MEXT and the Computational Materials Science Initiative (CMSI), Japan. The calculations in this work were carried out at the supercomputer center in the NIMS, ISSP and ITC (Oakleaf-FX) in the University of Tokyo, Kyushu University as well as the K computer at the RIKEN AICS through the HPCI Systems Research Projects. ZF is grateful for access to the computing and storage facilities owned by the parties and projects contributing to the National Grid Infrastructure MetaCentrum, Czech Republic, provided under the program "Projects of Large Infrastructure for Research, Development, and Innovations" (LM2010005).

## References

- 1 R. A. Marcus, *Ann. Rev. Phys. Chem.*, 1964, **15**, 155–196.
- 2 R. A. Marcus, *J. Chem. Phys.*, 1965, **43**, 679–701.
- 3 J. R. Miller, L. T. Calcaterra and G. L. Closs, *J. Am. Chem. Soc.*, 1984, **106**, 3047–3049.
- 4 A. Warshel, *J. Phys. Chem.*, 1982, **86**, 2218–2224.
- 5 A. Warshel, *Nature*, 1976, **260**, 679–683.
- 6 R. A. Kuharski, J. S. Bader, D. Chandler, M. Sprik, M. L. Klein and R. W. Impey, *J. Chem. Phys.*, 1988, **89**, 3248.
- 7 A. Warshel and W. W. Parson, *Annu. Rev. Phys. Chem.*, 1991, **42**, 279–309.
- 8 C. Hartnig and M. T. M. Koper, *J. Chem. Phys.*, 2001, **115**, 8540–8546.
- 9 J.-K. Hwang and A. Warshel, *J. Am. Chem. Soc.*, 1987, **109**, 715–720.
- 10 G. King and A. Warshel, *J. Chem. Phys.*, 1990, **93**, 8682–8692.
- 11 K. Ando, *J. Chem. Phys.*, 2001, **115**, 5228–5237.
- 12 D. W. Small, D. V. Matyushov and G. A. Voth, *J. Am. Chem. Soc.*, 2003, **125**, 7470–7478.

	Fe low spin		Fe high spin	
	M. Embd.	E. Embd.	M. Embd.	E. Embd.
$\Delta A$	-1.19	-1.18	-0.82	-0.70
$\lambda$	4.13	4.14	4.23	4.34
$\Delta A^\ddagger$	0.52	0.53	0.69	0.76

**Table 2** Difference in ET free energy characteristics between low and high Fe spin state. All quantities were calculated on optimized structures with  $20$  Å distance between the Ru and Fe cations. Total  $d$ -QM/MM energies were used to evaluate of ionization potentials and electron affinities. Both mechanical embedding and electrostatic embedding results are shown for comparison.

- 13 I. Tavernelli, R. Vuilleumier and M. Sprik, *Phys. Rev. Lett.*, 2002, **88**, 213002.
- 14 Y. Tateyama, J. Blumberger, M. Sprik and I. Tavernelli, *J. Chem. Phys.*, 2005, **122**, 234505.
- 15 J. Blumberger and M. Sprik, *J. Phys. Chem. B*, 2004, **108**, 6529–6535.
- 16 J. Blumberger, I. Tavernelli, M. L. Klein and M. Sprik, *J. Chem. Phys.*, 2006, **124**, 064507.
- 17 P. H.-L. Sit, M. Cococcioni and N. Marzari, *Phys. Rev. Lett.*, 2006, **97**, 028303.
- 18 Q. Wu and T. Van Voorhis, *Phys. Rev. A*, 2005, **72**, 024502.
- 19 H. Oberhofer and J. Blumberger, *J. Chem. Phys.*, 2009, **131**, 064101.
- 20 J. Blumberger and K. P. McKenna, *Phys. Chem. Chem. Phys.*, 2012, **15**, 2184–2196.
- 21 H. Nishioka and K. Ando, *J. Chem. Phys.*, 2011, **134**, 204109.
- 22 J. Blumberger, *Phys. Chem. Chem. Phys.*, 2008, **10**, 5651–5667.
- 23 X. Zeng, H. Hu, X. Hu, A. J. Cohen and W. Yang, *J. Chem. Phys.*, 2008, **128**, 124510.
- 24 Y. Kiyota, J.-y. Hasegawa, K. Fujimoto, B. Swerts and H. Nakatsuji, *J. Comput. Chem.*, 2009, **30**, 1351–1359.
- 25 Z.-K. Chu, G. Fu, W. Guo and X. Xu, *J. Phys. Chem.*, 2011, **115**, 14754–14761.
- 26 N. Asada, D. G. Fedorov, K. Kitaura, I. Nakanishi and K. M. J. Merz, *J. Phys. Chem. Lett.*, 2012, **3**, 2604–2610.
- 27 W. Böttcher, G. M. Brown and N. Sutin, *Inorg. Chem.*, 1979, **18**, 1447–1451.
- 28 J. S. Bader, R. A. Kuharski and D. Chandler, *J. Chem. Phys.*, 1990, **93**, 230–236.
- 29 K. M. Rosso and J. R. Rustad, *J. Phys. Chem. A*, 2000, **204**, 6718–6725.
- 30 A. Warshel and M. Levit, *J. Mol. Biol.*, 1976, **103**, 227–249.
- 31 S. Dapprich, I. Komaromi, K. S. Byun, K. Morokuma and M. Frisch, *J. Mol. Struct. Theochem*, 1999, **461–462**, 1–21.
- 32 R. A. Marcus, *J. Chem. Phys.*, 1956, **24**, 966–978.
- 33 R. A. Marcus, *J. Chem. Phys.*, 1956, **24**, 979–989.
- 34 S. Lee and J. T. Hynes, *J. Chem. Phys.*, 1988, **88**, 6853–6862.
- 35 M. D. Newton and H. L. Friedman, *J. Chem. Phys.*, 1988, **88**, 4460–4472.
- 36 H. J. Kim and J. T. Hynes, *J. Chem. Phys.*, 1990, **93**, 5194–5210.
- 37 M. Tachiya, *J. Phys. Chem.*, 1993, **97**, 5911–5916.
- 38 Y.-P. Liu and M. D. Newton, *J. Phys. Chem.*, 1994, **98**, 7162–7169.
- 39 D. V. Matyushov, *J. Chem. Phys.*, 2004, **120**, 7532–7556.
- 40 A. Farazdel, M. Dupuis, E. Michel and A. Aviram, *J. Am. Chem. Soc.*, 1990, **112**, 4206–4214.
- 41 W. L. Jorgensen, J. Chandrasekhar, J. D. Madura, R. W. Impey and M. L. Klein, *J. Chem. Phys.*, 1983, **79**, 926–935.
- 42 D. Andrae, U. Häussermann, M. Dolg, H. Stoll and H. Preuß, *Theor. Chim. Acta*, 1990, **77**, 123–14.
- 43 D. Andrae, U. Häussermann, M. Dolg, H. Stoll and H. Preuß, *Theor. Chim. Acta*, 1991, **78**, 247–266.
- 44 A. Bergner, M. Dolg, W. Kuechle, H. Stoll and H. Preuss, *Mol. Phys.*, 1993, **80**, 1431.
- 45 J. Wang, R. M. Wolf, J. W. Caldwell, P. A. Kollman and D. A. Case, *J. Comput. Chem.*, 2004, **25**, 1157–1174.
- 46 C. I. Bayly, P. Cieplak, W. Cornell and P. A. Kollman, *J. Phys. Chem.*, 1993, **97**, 10269–10280.
- 47 W. D. Cornell, P. Cieplak, C. I. Bayly and P. A. Kollman, *J. Am. Chem. Soc.*, 1993, **115**, 9620–9631.
- 48 M. J. Frisch, G. W. Trucks, H. B. Schlegel, G. E. Scuseria, M. A. Robb, J. R. Cheeseman, G. Scalmani, V. Barone, B. Mennucci, G. A. Petersson, H. Nakatsuji, M. Caricato, X. Li, H. P. Hratchian, A. F. Izmaylov, J. Bloino, G. Zheng, J. L. Sonnenberg, M. Hada, M. Ehara, K. Toyota, R. Fukuda, J. Hasegawa, M. Ishida, T. Nakajima, Y. Honda, O. Kitao, H. Nakai, T. Vreven, J. A. Montgomery, Jr., J. E. Peralta, F. Ogliaro, M. Bearpark, J. J. Heyd, E. Brothers, K. N. Kudin, V. N. Staroverov, R. Kobayashi, J. Normand, K. Raghavachari, A. Rendell, J. C. Burant, S. S. Iyengar, J. Tomasi, M. Cossi, N. Rega, J. M. Millam, M. Klene, J. E. Knox, J. B. Cross, V. Bakken, C. Adamo, J. Jaramillo, R. Gomperts, R. E. Stratmann, O. Yazyev, A. J. Austin, R. Cammi, C. Pomelli, J. W. Ochterski, R. L. Martin, K. Morokuma, V. G. Zakrzewski, G. A. Voth, P. Salvador, J. J. Dannenberg, S. Dapprich, A. D. Daniels, Ö. Farkas, J. B. Foresman, J. V. Ortiz, J. Cioslowski and D. J. Fox, *Gaussian 09, Revision A.1*, 2009.
- 49 D. A. Case, T. A. Darden, T. E. Cheatham, C. L. Simmerling, J. Wang, R. E. Duke, R. Luo, R. C. Walker, W. Zhang, K. M. Merz, B. Roberts, B. Wang, S. Hayik, A. Roitberg, G. Seabra, I. Kolossvary, K. F. Wong, F. Paesani, J. Vanicek, J. Liu, X. Wu, S. Brozell, T. Steinbrecher, H. Gohlke, Q. Cai, X. Ye, J. Wang, M.-J. Hsieh, G. Cui, D. R. Roe, D. H. Mathews, M. G. Seetin, C. Sagui, V. Babin, T. Luchko, S. Gusarov, A. Kovalenko and P. A. Kollman, *Amber 11*, University of California, San Francisco, 2010.
- 50 J. Blumberger and G. Lamoureux, *Mol. Phys.*, 2008, **106**, 1597–1611.
- 51 L.-P. Wang and T. Van Voorhis, *J. Chem. Theory Comput.*, 2012, **8**, 610–617.
- 52 A. Warshel and J.-K. Hwang, *J. Chem. Phys.*, 1986, **84**, 4938–4957.
- 53 J.-K. Hwang, G. King, S. Creighton and A. Warshel, *J. Am. Chem. Soc.*, 1988, **110**, 5297–5311.
- 54 Q. Wu and T. Van Voorhis, *J. Chem. Theory Comput.*, 2006, **2**, 765–774.
- 55 P. Delahay, *Chem. Phys. Lett.*, 1982, **87**, 607–611.
- 56 K. Ando, *J. Chem. Phys.*, 2001, **114**, 9470–9477.
- 57 P. Delahay, K. Von Burg and A. Dziedzic, *Chem. Phys. Lett.*, 1981, **79**, 157–161.
- 58 H. Oberhofer and J. Blumberger, *Angew. Chem. Int. Ed.*, 2010, **49**, 3631–3634.
- 59 H. Oberhofer and J. Blumberger, *J. Chem. Phys.*, 2010, **133**, 244105.
- 60 H. Iikura, T. Tsuneda, T. Yanai and K. Hirao, *J. Chem. Phys.*, 2001, **115**, 3540–3544.
- 61 J.-D. Chai and M. Head-Gordon, *Phys. Chem. Chem. Phys.*, 2008, **10**, 6615–6620.
- 62 T. Stein, H. Eisenberg, L. Kronik and R. Baer, *Phys. Rev. Lett.*, 2010, **105**, 266802.